Properties and structure of the F-doped (Bi,Pb)-Sr-Ca-Cu-O superconductor

Xiao-hui Gao
Applied Quantum Research Center, Central South University of Technology, Changsha, Hunan 410083, China

Xiao-Gang Wang
Department of Physics, Hunan Normal University, Changsha, Hunan 410006, China

Shu-fen Jiang and Jie Li
Applied Quantum Research Center, Central South University of Technology, Changsha, Hunan 410083, China

Sai Gao and Guo-dong Zheng
Department of Chemistry, Jilin University, Changchun 130023, China
(Received 10 January 1994)

Using transmission electron microscopy, x-ray photoelectron spectroscopy, infrared, positron annihilation, and differential specific-heat measurements, we have studied the properties and structure of the F-doped (Bi,Pb)-Sr-Ca-Cu-O superconductor. The results show that the fluorine atoms are homogeneously distributed in the superconducting phase and substituted for the oxygen atoms at O(2) crystallographic sites; the Pb-F and Cu-F bonds are formed. F-doping results in the variance of the incommensurate modulation structure, the increase of the point defects and chemical pressure, the enhancement of the flux-pinning effect, and the change of the electronic structure and chemical bond, and greatly improves the superconductive properties of the 2223 phase of (Bi,Pb)-Sr-Ca-Cu-O.

I. INTRODUCTION

A significant T_c enhancement in Bi-based 2223 phase superconductors by a partial substitution of fluorine for oxygen has been reported.[1-3] Gao *et al.*[3] studied some characteristics of the F-doped Bi-based superconductors, and found that these superconductors have a slower flux-creep rate and obviously produce the flux-pinning effect. However, the crystallographic site of the doped fluorine and its influence on superconducting properties were not clearly known until now. In this paper, we present the results from transmission electron microscopy (TEM), x-ray photoelectron spectroscopy (XPS), infrared (IR), positron annihilation, and differential specific-heat measurements, and discuss the possible location of the doped fluorine and the physical behaviors caused by F doping.

II. SAMPLE PREPARATION

To study the structure and properties of superconductor, a single crystal or single phase is important for measurement. Whereas, as pointed out in Refs. 4 and 5, the pure 2223 phase Bi system sample cannot be obtained easily. The principal difficulty is due to the coexistence of the 2223 phase with the 2212 phase in samples. Thus, undoped reference sample A and F-doped sample B were prepared for the compared measurements to exclude the influence of the 2212 phase.

For sample A, according to nominal composition $Bi_{1.65}Pb_{0.35}Sr_2Ca_2Cu_3O_{10}$, high purity Bi_2O_3, PbO, $SrCO_3$, $CaCO_3$, and CuO were dissolved in 1:1 HNO_3 then dried at 120 °C, preheated at 760 °C for 6 h, when nitrate was transformed into oxides, taken out and ground, calcined at 810 °C for 12 h, cooled, and ground again. The powder was pressed into pellets ($\sim$12 mm in diameter and $\sim$1.2 mm thick). Then these pellets were sintered at 850 °C for 360 h and cooled naturally down to room temperature in the furnace. The zero resistance temperature T_{c0} was 108.6 K for the samples. $Q_{2223}=86.5\%$ was obtained; here, Q_{2223}, which presents the amount factor of the 2223 phase, could approximately be evaluated from Fig. 1 and the formula

$$Q_{2223}\% = A^{002}_{2223}(A^{002}_{2223}+A^{002}_{2212})^{-1}\% , \quad (1)$$

where A^{002}_{2223} is the area of the 002 peak for the 2223 phase in the x-ray diffraction (XRD) diffractogram and A^{002}_{2212} is that for the 2212 phase.

For sample B, except 0.4 mol CuF_2 replacing 0.4 mol CuO, other components are the same as sample A. The powder was homogeneously mixed by grinding, heated at a rate of 450 °C/h to 680 °C and then 12 °C/h to 750 °C, and remained at 750 °C for 12 h. The products were ground, pressed into pellets, sintered at 790 °C for 10 h and then at 835 °C for 160–180 h, and finally quenched in air. The R-T and AC-T curves of the sample B are shown in Fig. 2. We can see from Fig. 2 that the zero resistance temperature T_{co} is 116.4 K, and the diamagnetic behavior occurs at 117.2 K. $Q_{2223}=93\%$ was obtained from Fig. 1.

The XRD data show that the sample A and B were all tetragonal. Their lattice parameters were, respectively, $a=5.411$ Å and $c=37.246$ Å for sample A; $a=5.357$ Å and $c=36.951$ Å for sample B.

0163-1829/94/50(2)/1237(7)/$06.00

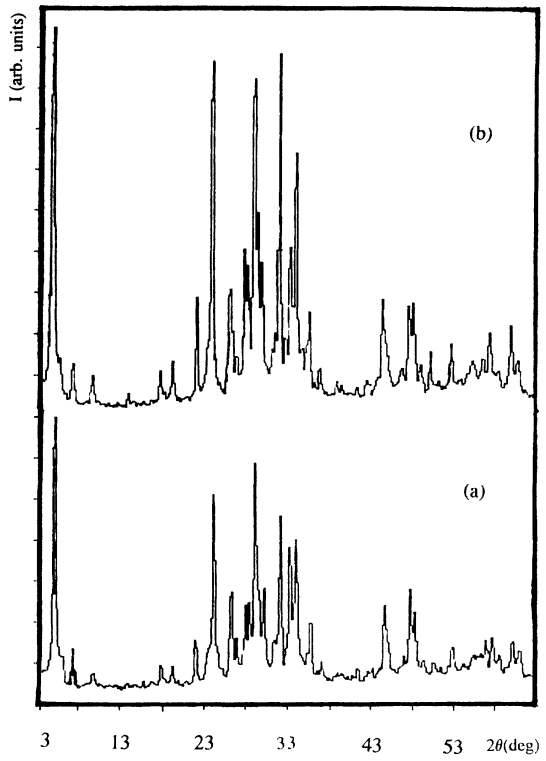

FIG. 1. X-ray-diffraction pattern for sample A and sample B. (a) for sample A, (b) for sample B.

III. MEASUREMENT RESULTS

A. Transmission electron microscopy (TEM) analysis

Presentation of incommensurate modulation structure is one of the features of Bi-based superconductors, the variation of which is an influence factor on T_c. Generally, doped elements make the modulation structure weaker and the period of the modulation longer. So by means of TEM analysis of the F-doped Bi-system superconductor, we can know whether F enters into the superconducting phase or not.

The H-800 TEM was used in the measurements. The diffraction patterns for samples A and B are shown in Fig. 3. From Fig. 3 we obtained the modulation periods at the b direction for the 2223 phase: 9.442 b for sample A, which is approximately consistent with the Ramesh's report (9.5 b),[6] and 13.880 b for sample B, which show that F doping obviously extends the period of the modulation. Figure 3 also indicates that the feature of modulation for sample B is more clear than that for sample A. The results are the direct evidence for the fact that F has entered into the superconducting phase.

B. X-ray photoelectron spectroscopy (XPS)

Since the discovery of Bi-system superconductors, some investigations about the chemical band and electronic structure of Bi-system superconductors by XPS have been reported.[6–8] Kihiki *et al.*[8] discussed the distribution and properties of Bi, Sr, and Ca in the crystals based on the XPS experiments. According to the XPS results, Kishida *et al.*[7] pointed out that the binding energy E_b of Cu $2p^{3/2}$ is stable whether in the Bi-Sr-Cu-O, (Bi,Pb)-Sr-Cu-O, (Bi,Pb)-Sr-Ca-Cu-O or Bi-Sr-Ca-Cu-O superconductor, but the E_b of Sr $3d^{5/2}$ and O $1s$ is vari-

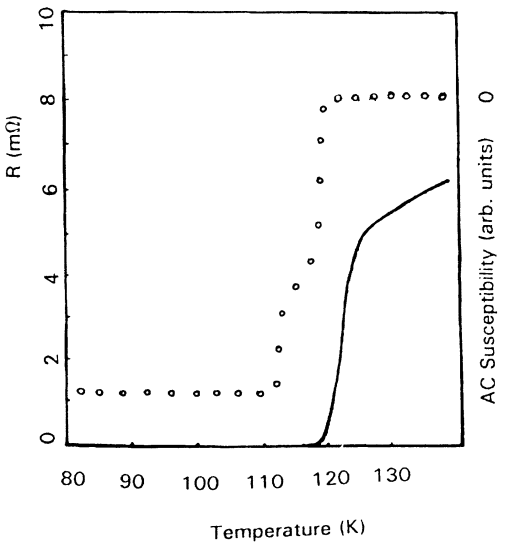

FIG. 2. Curve R-T and Ac-T for sample B.

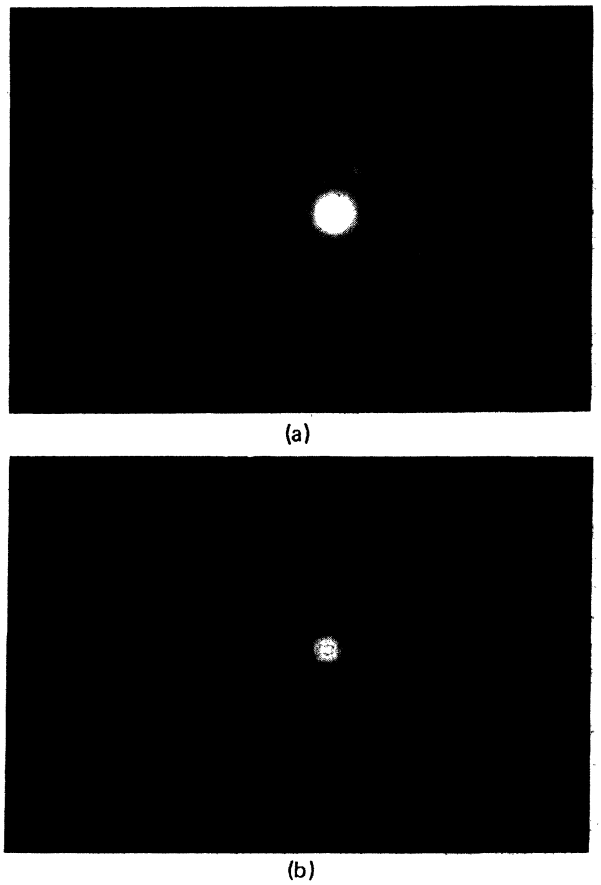

FIG. 3. Electronic-diffraction pattern for sample A and sample B. (a) for sample A, (b) for sample B.

able in the different systems. In this paper, we present results of XPS studies on the F-doped Bi-system superconductor and discuss the characteristic of the distribution and chemical bond of doped F.

XPS studies were carried out in a VG Silentific ESCA MK II system. The x-ray source was Mg$K\alpha$ and the vacuity was 1×10^{-8} mba. The charge effect was corrected by $C_{1s}=284.4$ eV. All measurements were performed at room temperature. The results displayed that the changes of only Pb $4f^{7/2}$ and Cu $2p^{3/2}$ were more than 0.3 eV. Their XPS spectra are illustrated in Fig. 4(I) and Fig. 4(II). The E_b of F 1s in sample B is the same as that of PbF_2 and CuF_2, which is equal to 684.3 eV. The results also show that the E_b for other elements in sample A is nearly identical with that in sample B.

Kishide *et al.*[7] reported that the E_b of Cu $2P^{3/2}$ in Bi-Sr-Cu-O, (Bi,Pb)-Sr-Cu-O, (Bi,Pb)-Sr-Ca-Cu-O, or Bi-Sr-Ca-Cu-O superconductor, is all equal to 934.0 eV, which is close to our result for sample A 934.4 eV as shown in Fig. 4(I). The error possibly origins from the different apparatus in both laboratory and the samples made under different conditions. Whereas, the E_b^B of Cu $2p^{3/2}$ for a F-doped sample B is equal to 935.1 eV, which is close to the E_b for pure CuF_2 935.4 eV. $E_b^B-E_b^A=0.70$ eV implies that the oxidation state of copper in sample B may be higher than that in sample A.

The E_b of Pb $4f^{7/2}$ in pure PbO is 138.0 eV, which is nearly equal to that 138.1 eV in Bi-based superconductors obtained by Gopinath and Subramanian.[4] The E_b of Pb $4f^{7/2}$ in sample A was also 138.1 eV as shown in Fig. 4(II). These indicate that the electronic state of lead is not a discrepancy in pure PbO and in the Bi-based superconductor. However, as shown in Fig. 4(II), the E_b of Pb $4f^{7/2}$ in sample B was 139.0 eV, which is identical with that in pure PbF_2. $E_b^B-E_b^A=0.9$ eV clearly shows that the valence electron distribution of Pb is violently influenced by fluorine in the F-doped (Bi,Pb)-Sr-Ca-Cu-O superconductor.

It is generally believed that the site of Bi may be replaced by Pb in the Pb-doped Bi-system superconductor. Therefore, the above results manifest that the fluorine not only exists in the 2223 phase but also selectively interacts with copper and lead in the F-doped (Bi,Pb)-Sr-Ca-Cu-O superconductor.

C. IR spectra

The 2212 and 2223 Bi-based superconductors have identical symmetry. They belong to the D_{4h}^{17} space group. It is not difficult to appoint the normal vibration and the jurisdiction of irreducible representation in Bi-based superconductors.[9-11] But in a doped system such as the replacement of Bi by 0.4 mol lead, only some unit cells can include one lead atom, and when there is a lead atom substituted for a bismuth atom in the unit cell, the symmetry would be decreased; thus because the dopant makes the chemical circumstance change, the number of IR peaks will increase, and some IR peaks will be shifted. Hence, IR spectrum for the doped system would be the superposition of the IR peaks from the unit cells with the different composition and symmetry. In this section, we focus the investigation on whether fluorine enters into the superconductive phase or not and which kind of place it occupies. We measured the standard materials such as CuF_2, PbF_2, CaF_2, and SrF_2, etc., the undoped and F-doped (Bi,Pb)-system superconductive sample under the same condition, and then analyzed and made a comparison among the results.

Since some normal vibration is very weak in the (Bi,Pb)-system superconductor and the samples are very black, the IR-photophonon spectrum technology was used to raise sensitivity. A Nicolet 5PC equipment was employed to perform all measurements by scanning from 4000 to 240 cm^{-1}. The peaks for the samples mainly ap-

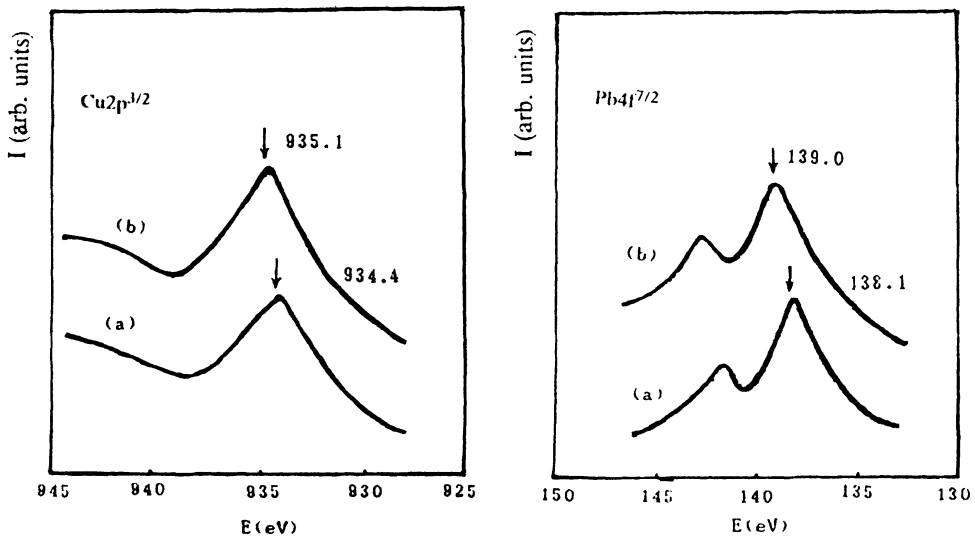

(I) (II)

FIG. 4. XPS spectra for sample A and sample B.

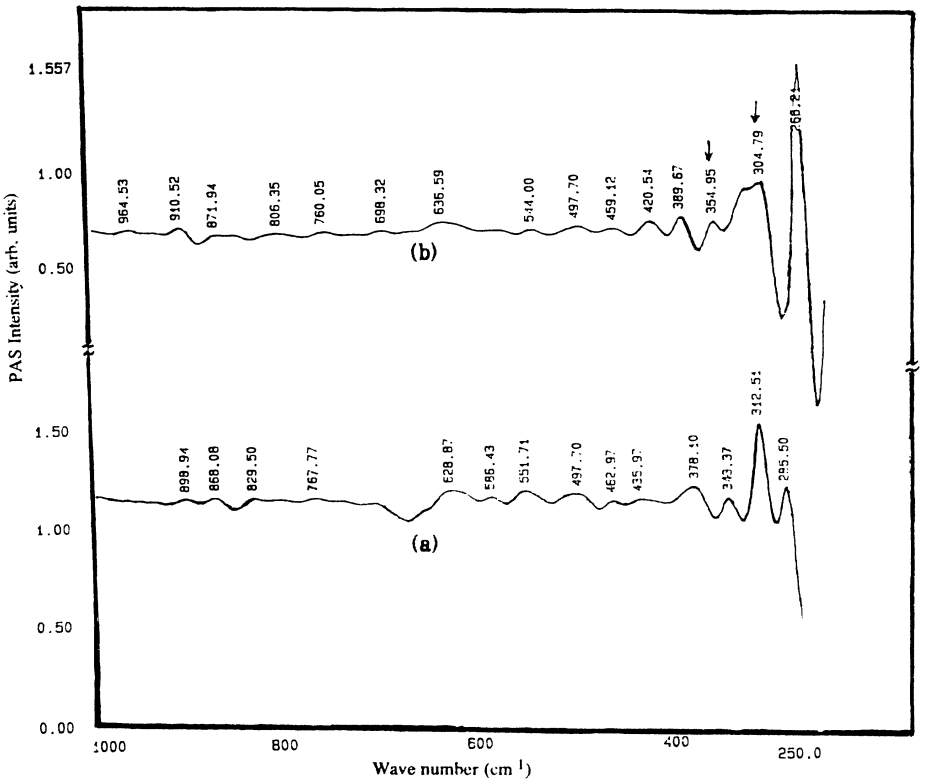

FIG. 5. IR spectra. (a) for sample *A*, (b) for sample *B*.

peared in the range of 1000–240 cm^{-1}, as shown in Fig. 5. We find that in sample *B*, the Pb-F and Cu-F peaks appeared at 304.79 cm^{-1} and 354.95 cm^{-1}, respectively, and other metallic fluoride vibration peaks did not appear. The results show that the fluorine not only enters into the superconducting phase, but also is bonded to lead and copper.

D. Specific heat

The differential specific heat can reflect bulk superconducting behaviors of the sample. In this section, the differential specific-heat measurements were used to study whether fluorine enters into the superconducting phase or not, and the effect of fluorine on superconductivity. A 342.0±0.2 mg of sample *B* and the same weight of sample *A* were taken and the measurements were carried out in the temperature range between 80–150 K.

The results are shown in Fig. 6. From Fig. 6, we can see that the T_c of sample *B* is 7 K higher than that of sample *A*, which implies that fluorine enters into the superconducting phase. The big and sharp specific-heat anomalous peak of curve (b) in Fig. 6 shows that the fluorine distribution in sample *B* is homogeneous, otherwise the shoulder peaks or wide peak will appear in the curve. In addition, bigger curvature of curve (b) implies that F-doped samples have a higher Debye temperature.

E. Positron annihilation study

Positron annihilation spectroscopy (PAS) is a useful method in the study of electronic structures and defects of condensed matter, which has been widely used to study Bi-based superconductors.[12–14] In this section, we report some PAS results about the F-doped Bi-based superconductor.

Positron lifetime spectra were obtained by an ORTEC fast-fast coincidence system. The resolution [full width at half maximum (FWHM)] was determined to be 225 ps. A 20 μCi ^{22}Na sandwich source with a Mylar film substrate was used. Each lifetime spectrum was accumulated to 2×10^6 counts. The lifetime spectra were analyzed by the program POSITRONFIT-EXTENDED,[15] and were freely fitted to three components, subtracting a source component ($\tau=310$ ps, $I=15\%$), which is primarily due to positron annihilation in NaCl and Mylar film.

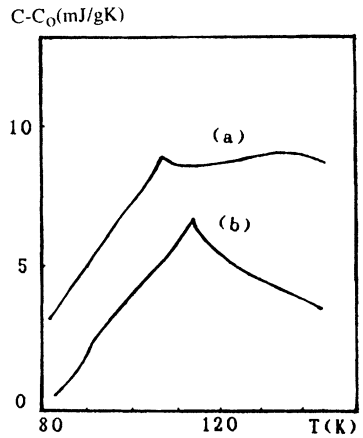

FIG. 6. Specific-heat curve. (a) for sample *A*, (b) for sample *B*.

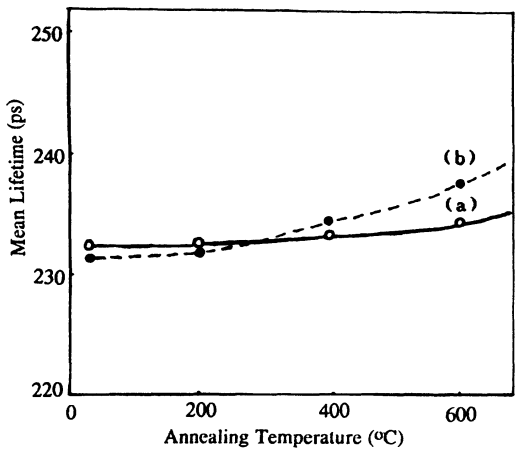

FIG. 7. Variation of mean lifetime as a function of annealing temperature. (a) for sample A, (b) for sample B.

The mean lifetime τ_m is obtained as

$$\tau_m=(\tau_1 I_1+\tau_2 I_2)/(I_1+I_2)\ . \tag{2}$$

Here I_1 and I_2 are the intensity of the lifetime τ_1 and τ_2. The experiments showed that the longest lifetime τ_3 and its intensity I_3 had nothing to do with the properties of samples; therefore, we do not discuss this component here.

The measurements showed that τ_m of samples was independent of the temperature below 300 K, but was a function of the annealing temperature of the samples. Here, the annealing temperature varied from 800–200 °C, and at each temperature point, the samples were heated in air for 1 h and quenched onto a large cold copper plate. The results are shown in Fig. 7. The mean lifetime of sample B is shorter than that of sample A when the annealing temperature is lower than 200 °C, whereas, when the annealing temperature is higher than 300 °C, the mean lifetime becomes larger than that of sample A, as shown in Fig. 7. It means that fluorine is responsible for the variance of the means lifetime τ_m.

The Doppler-broadening annihilation radiation (DBAR) spectra were obtained by a coaxial high pure Ge detector with a resolution (FWHM) of 1.5 keV at 514 keV line of ^{85}Sr. A 5 μCi ^{22}Na sandwich source with an Ni foil substrate was used. Each spectrum was accumulated to 5×10^6 counts.

The full width at half maximum (FWHM) of every DBAR spectrum after deconvolution is summarized in Table I. The deconvolution spectra of sample B in normal and superconducting states are shown in Fig. 8. The difference spectra of samples A and B were obtained by subtracting the normal-state spectrum from the superconducting state spectrum, which is shown in Fig. 9. As

TABLE I. FWHM (keV) of DBAR spectra for samples A and B.

Samples	N state	S state	N-S state
A	3.02	3.06	0.04
B	2.96	3.06	0.10

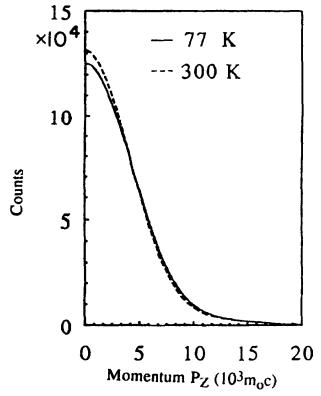

FIG. 8. Positron DBAR deconvolution spectra for sample B in N and S states.

seen in Table I the FWHM of superconducting state is larger than that of normal state for each sample. The DBAR spectrum becomes sharper near $P_z=0$ at 300 K as shown in Fig. 8. There is no sharp cutoff in the spectra to indicate a Fermi momentum. The sharpening of DBAR spectra with increasing temperature is contrary to what is commonly observed in positron annihilation. Normally, the thermal motion of the positron and electron increases with temperature and adds to the width of the DBAR spectra. From Fig. 9, we can see that the difference spectra is negative at the low momentum region, whereas it is positive at the high-momentum region. These results indicate that the number of electrons with high-momentum increases at liquid-nitrogen temperature. From Fig. 9, a very interesting result can be seen; namely, the amplitude of the negative peak near $P_z=0$ for sample B is about twice that of sample A. Since the area of the positive or negative region in a spectrum is related to the amount of charge transfer, the above result implies that F doping can greatly change the amount of charge transfer.

IV. DISCUSSION AND CONCLUSION

A. The crystallographic sites of fluorine

The x-ray diffraction results show that the content of other phases is about 7%, the 2223 superconducting

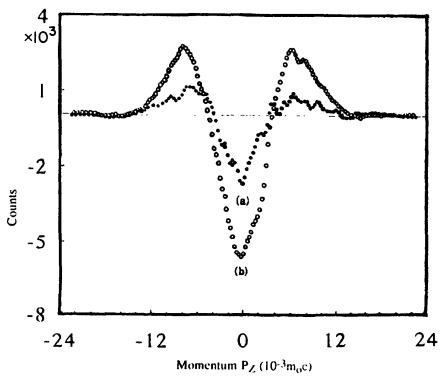

FIG. 9. Positron DBAR difference spectra of N and S states. (a) for sample a, (b) for sample B.

phase is the main compound, and there is no metallic fluoride or other impurity in sample *B*. The TEM analysis and specific-heat measurement indicate that the fluorine has entered into the superconducting phase. XPS and IR spectra further indicate that fluorine is bonded to lead and copper. So, we can conclude that the fluorine really enters into the superconducting phase.

The further problem is which site is occupied by fluorine in the unit cell. For this reason, we first point out that the nominal composition of fluorine was equal to 0.8 mol introduced by CuF_2, and because CuF_2 is unstable at higher temperature, the reaction $2\ CuF_2+O_2 \rightarrow 2CuO+2F_2\uparrow$ will happen and some fluorine will run away during calcining and sintering; the quantity of escaping fluorine increases with the increase of temperature and time. Elemental analysis results showed that sintering 200 h at 825 °C, the amount of fluorine in sample *B* was lower than or equal to 0.25 mol, which implies that there would be less than one fluorine atom in every unit cell on an average. Moreover, XPS and IR display that there exist chemical bonds of Pb-F and Cu-F in sample *B*, so we can predicate that the fluorine is bonded to Pb and Cu simultaneously, otherwise, it will contradict with our experimental results as TEM analysis, x-ray diffraction, and specific heat, etc. Generally, the site of Bi is occupied by Pb in Pb-doped Bi-based superconductors. So the O(2) crystallographic site may be replaced by the fluorine atom as shown in Fig. 10, which is similar to what the O(4) site is replaced by the fluorine atom in the F-doped Y-Ba-Cu-O and R-Ba-Cu-O.[16,17]

In the Bi-based superconductors, copper bonded to four O(1) to form the copper-oxide plane, and to O(2) to construct a pyramid. Since F at the O(2) site bonded to Cu produces a strong Jahn-Teller effect, the fluorine would approach to lead, which may have a relation to the XPS experiments which showed that the binding energy shift of Pb $4p^{7/2}$ was bigger than that of Cu $2p^{3/2}$, and the IR spectra which indicate the wave-number order of Cu-F and Pb-F.

Bond energy $D(M-L)$ and force constant K_{ML} between atom M and L can be evaluated by the following formulas:[18,19]

$$D(M-L)=[D(M-M)D(L-L)]^{1/2} + \frac{X_L-X_M}{X_L+X_M}E_L\ , \tag{3}$$

$$K_{ML}=(K_M K_L)^{1/2}+\frac{4.612(X_L-X_M)}{R^3(X_L+X_M)}\ . \tag{4}$$

Here the X_M is the atomic electronegativity of atom M, E_L is the electronic affinity of atom L, and R_{ML} is the distance between atom L and M. The results are listed in Table II. We can see from Table II that the Cu-F and Pb-F bonds produced by the substitution of F for O(2) are stronger than the Cu-O and Pb-O bonds in the undoped (Bi,PB)-system superconductor, which makes the distance between the CuO_2 layer and $Bi(Pb)O_2$ layer contract and the *c* axis of the unit cell shorten. On the other hand, as more charges are transferred from Cu and Pb to fluorine that to O(2), which enhances the positive valences of these metallic elements, the attraction between the metallic ions and ligand is strengthened, which makes the *a* and *b* axes contract. Based on the above discussion, we can conclude that with the substitution of F for O(2), the unit cells contract, some chemical bonds strengthen, the volume of the unit cell reduces, and the notable chemical press is produced.

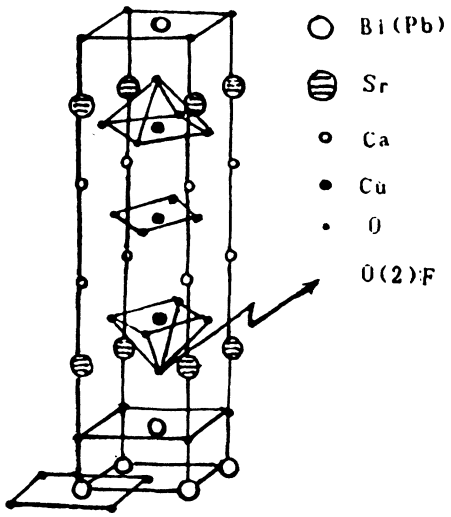

FIG. 10. Crystallographic site of fluorine in unit cell.

B. Mechanism for the enhancement of T_c

Many researchers have pointed out that the T_c may be raised with the increase of chemical pressure in high-T_c superconducting metallic oxide. The experiments showed the ratio of the unit-cell volume for the F-doped sample to that for the undoped sample V_F/V_0 was 0.9727. It implies that F doping would make the chemical pressure increase, and hence enhances T_c of the superconductor.

It is generally thought that the Bi-O layers are electron reservoirs and the Cu-O layers are superconducting charge carriers. The O(2) site replaced by F is just located at an important position which links the Bi-O layer to the Cu-O layer, and can affect the transfer properties of

TABLE II. The bond energy and force constant of Cu-F and Pb-F bond. The subscript *e* for experimental value and *c* for calculated value by formulas (3) and (4).

$D(\text{O-O})_e$	$D(\text{F-F})_e$	$D(\text{Pb-Pb})_e$	$D(\text{Cu-Cu})_e$	$D(\text{Cu-O})_c$	$D(\text{Pb-O})_c$	$D(\text{Cu-F})_c$	$D(\text{Pb-F})_c$	E_0	E_F
33.2	36.6	14.0	8.0	38.31	38.56	50.35	55.87	2.30	3.80
$K(\text{O-O})_e$	$k(\text{F-F})_e$	$k(\text{Pb-Pb})_e$	$k(\text{Cu-Cu})_e$	$k(\text{Cu-O})_c$	$k(\text{Pb-O})_c$	$k(\text{Cu-F})_c$	$k(\text{Pb-F})_c$		
3.83	4.45	0.40	0.20	0.98	1.35	1.07	1.46		

the carrier. The positron DBAR spectra indicate that F doping can greatly change the amount of charge transfer, which may make the carrier concentration change to its optimum and hence increase the T_c.

We[20] calculated the electronic structure of the F-doped (Bi,Pb)-system superconductor by the DV-$X\alpha$ method and found that when fluorine replaced O(2), the O $2p$ hole concentration in the Cu-O layer increased. The XPS results also show that the positive valence of copper in the F-doped sample increased, which induced the population to decrease in p orbitals of the oxygen atom, the hole concentration to increase, and thus the T_c to be improved.

In addition, the increase of the anomalous specific-heat sharp peak for the F-doped sample indicates that there was a high Debye frequency, so the phonon energy from lattice vibration increases, and the electrons exchange energy with a high-energy phonon, which leads to the increase of the energy gap when the Cooper electron pair was formed according to BCS theory. The results imply that there are more stable Cooper electron pairs in the F-doped sample than in the undoped sample, and the superconducting current density is bigger in the former than in the latter.

As described above, since lead and fluorine are simultaneously doped in Bi-based superconductor, the symmetry is decreased, and the degenerate energy level in the valency band as well as the Fermi level is split, so the state density will increase in the Fermi surface, which profits T_c increasing. In summary, we conclude that the increase of the T_c belongs to nature in the F-doped superconductor.

C. The behavior in magnetic field

We investigated the magnetization irreversibility lines under a 0–2400 O_e magnetic field for the quenched F-doped (Bi,Pb)-system superconductor.[3] An interesting phenomenon was that the flux-creep rate $S = dM/d\ \ln t$ for the F-doped sample became slower, the $S \propto H^2$ for (Bi,Pb)-Sr-Ca-Cu-O, and the $S \propto H^{1/2}$ for (Bi,Pb)-Sr-Ca-Cu-(O,F). It was estimated that the flux-pinning potential was about 3000 K. These experimental facts probably come from two aspects; first, lightly doped fluorine atoms may be the pinning center, and secondly, since the positron mean lifetime of the F-doped sample is larger than that of the undoped sample when the quenching temperature is higher than 300 °C as shown in Fig. 7, which means that more point defects were produced in the F-doped sample, the additional pinning centers were formed. Therefore, the results of the increase of the pinning potential and the decrease of the flux-creep rate are inevitable. It is worth pointing out that the T_c of the F-doped sample quenched in the air increased 2.5±0.5 K higher than that of the same sample cooled in the furnace, which may be correlated to the pinning effect.

[1] X. H. Gao, X. L. Wu, H. Yan, and Z. L. Yin, Mod. Phys. Lett. B **4**, 137 (1990).

[2] S. Lee and S. S. Horiuchi, Physica C **185-189**, 477 (1991).

[3] X. H. Gao, J. Li, De Gao, G. D. Zheng, and S. Gao, Mod. Phys. Lett. B **6**, 443 (1992).

[4] C. S. Gopinath and S. Subramanian, Physica C **176**, 331 (1991).

[5] M. Pissos, V. Psycharis, and D. Niarchos, Physica C **185-189**, 485 (1991).

[6] R. Ramesh, M. S. Hegde, C. C. Chang, J. M. Jarascon, S. M. Green, and H. L. Luo, J. Appl. Phys. **66**, 4878 (1989).

[7] S. Kishida, H. Tokutaka, W. Futo, H. Fujimoto, K. Nishimari, and N. Ishihara, Jpn. J. Appl. Phys. **30**, 926 (1991).

[8] S. Kihiki, T. Wada, S. Kawashima, H. Takagi, S. Uchida, and S. Tanaka, Phys. Rev. B **38**, 8868 (1988).

[9] E. O. Piro, J. A. Guüda, N. E. Massa, and P. J. Aymonio, Phys. Rev. B **39**, 7255 (1989).

[10] S. Mase and T. Yasuda, Jpn. J. Phys. Soc. **58**, 658 (1989).

[11] T. Kajitani, K. Kusaba, M. Kikuchi, N. Kobayashi, Y. Syono, T. B. Williams, and M. Hirabayashi, Jpn. J. Appl. Phys. **27**, 587 (1988).

[12] C. S. Sundar, A. Bharathi, W. Y. Ching, Y. C. Jean, P. H. Hor, R. L. Meng, Z. J. Huang, and C. W. Chu, Phys. Rev. B **43**, 13 019 (1991).

[13] Y. C. Jean, C. S. Sunder, A. Bharathi, J. Kyle, H. Nakanishi, P. K. Tseng, P. H. Hor, R. L. Meng, Z. J. Huang, C. W. Chu, Z. Z. Wang, P. E. Turchi, R. H. Howell, A. L. Wachs, and M. J. Fluss, Phys. Rev. Lett. **64**, 1593 (1990).

[14] A. Bharathi, C. S. Sunder, W. Y. Ching, Y. C. Jean, P. H. Hor, Y. Y. Xue, and C. W. Chu, Phys. Rev. B **42**, 10 199 (1990).

[15] P. Kirkegaard and M. Eldrup, Comput. Phys. Commun. **7**, 401 (1977).

[16] X. H. Gao, H. Yan, Z. L. Yin, and X. L. Wu, Chin. J. Chem. Phys. **3**, 57 (1990).

[17] H. P. Li and X. H. Gao, Acta Phys. Sin. **41**, 851 (1992).

[18] X. H. Gao and T. L. Chen, Kexue Tong Bao **26**, 141 (1981).

[19] X. H. Gao and T. L. Chen, Chin. J. Nature **3**, 635 (1980).

[20] H. L. Liu, N. Y. Chen, and X. H. Gao, Chin. J. Chem. Phys. **5**, 98 (1992).

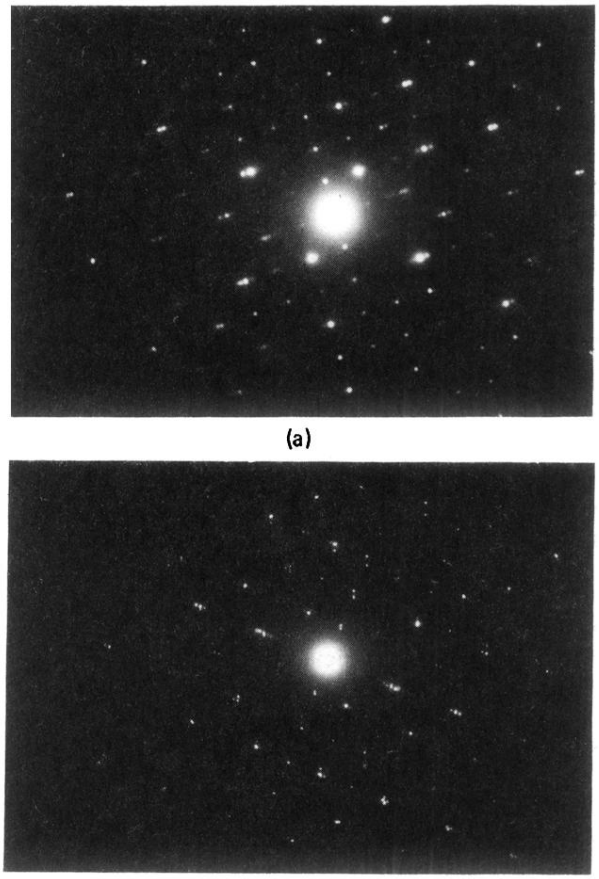

FIG. 3. Electronic-diffraction pattern for sample A and sample B. (a) for sample A, (b) for sample B.